

ac-driven atomic quantum motor

A. V. Ponomarev, S. Denisov, and P. Hänggi

Institute of Physics, University of Augsburg, Universitätstr. 1, D-86159 Augsburg

(Dated: October 23, 2019)

We invent an ac-driven quantum motor consisting of two different, interacting ultracold atoms placed into a ring-shaped optical lattice and submerged in a pulsating magnetic field. While the first atom carries a current, the second one serves as a quantum starter. For fixed zero-momentum initial conditions the asymptotic carrier velocity converges to a unique non-zero value. We also demonstrate that this quantum motor performs work against a constant load.

PACS numbers: 05.60.-k, 37.10.Jk, 84.50.+d

Linear or rotational motion presents the basic working principle powering all sorts of machines. Since almost two centuries ago, after the invention of the first electrical motor [1], the ever continuing miniaturization of devices has profound consequences for several branches of science, industry, and everyday life. This process has already passed the scale of micrometers [2] and has entered the realm of the world of nanoscale [3]. Bioinspired devices such as chemical or light driven synthetic molecular motors identify just one of those recent successes [4]. While the operational description of such molecular motors mainly rests on classical concepts, much less is known for operational schemes that are *fully* quantum mechanical in nature. An ideal resource for the latter possibility is the dynamics of cold atoms that are positioned in optical potentials [5].

With this work, we put forward a setup for a quantum motor which consists of two species of interacting, distinguishable quantum particles that are loaded into a ring-shaped optical potential. The blueprint for such an underlying ring-shaped one-dimensional optical lattice has been proposed recently [6] and a first experimental realization has been reported in [7]. Here, we employ this setup to devise an engine which works as a genuine ac-driven quantum motor. Moreover we discuss parameter values suitable for the realization of the quantum engine with present-day available experimental setups.

ac-quantum motor.—Figure 1 outlines our device. The ring-shaped optical potential, which results either from the interference of a Laguerre-Gauss (LG) laser beam with a plane wave [6] or, alternatively, of two collinear LG beams with different frequencies [7] is capable of trapping two interacting atoms. One of the atoms, termed “carrier”, c , is driven by an external field, while the other atom, termed “starter”, s , interacts locally via elastic s-wave collisions with the “carrier”, but remains unaffected by the driving field [8]. Two possible setups that come to mind are: (i) A neutral “starter” and an ionized “carrier”, a suitable driving field can be implemented in a way typically done for electrons placed in a conducting ring, i.e., by a time-dependent magnetic flux threading the lattice [9]. (ii) A spinless “starter” and a “carrier”-atom with a non-zero spin which is driven by

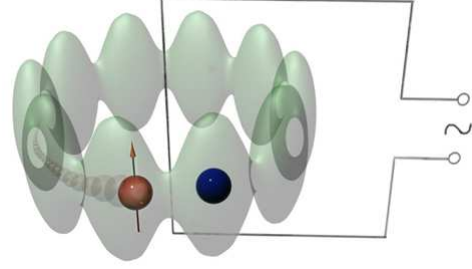


FIG. 1: (color online) Atomic quantum motor: Two different ultracold atoms are loaded into a ring-shaped optical lattice. Both atoms interact locally with each other, while only one carrier (the one with an arrow) is magnetically powered.

a time-dependent cone-shaped magnetic field of a Ioffe-Pritchard trap [6, 10].

We next assume that both atoms are loaded into the lowest energyband of a deep, ring-shaped optical potential with L lattice sites. Specifically, the potential amplitude $V_0 \gtrsim 5E_0$, where $E_0 = \hbar^2\pi^2/2Md^2$ is the “recoil” energy, M is the mass of the atom, and d is the lattice constant [5]. The time-dependent homogeneous vector potential $A(t)$ does not induce any appreciable transitions between the ground band and the excited band(s).

The ac-driven, total Hamiltonian H_{tot} of the the motor

$$H_{\text{tot}} = H_c(t) + H_s + H_{\text{int}}, \quad (1)$$

is composed of the time-dependent Hamiltonian H_c for the “carrier”

$$H_c(t) = -\frac{J_c}{2} \left(\sum_{l_c=1}^L e^{iA(t)} |l_c+1\rangle \langle l_c| + \text{H.c.} \right) \otimes \mathbf{1}_s, \quad (2)$$

and for the “starter” H_s , respectively, i.e.,

$$H_s = -\frac{J_s}{2} \left(\sum_{l_s=1}^L |l_s+1\rangle \langle l_s| + \text{H.c.} \right) \otimes \mathbf{1}_c. \quad (3)$$

Here, J_c and J_s are the corresponding hopping strengths. At time t_0 , one suddenly switches on the ac-driving. This is incorporated with a time-periodic (for times $t \geq t_0$)

vector potential $A(t)$, to be further specified below. The salient carrier-starter (on-site)-interaction reads

$$H_{\text{int}} = W \sum_{l_c, l_s=1}^L \delta_{l_c, l_s} |l_c\rangle \langle l_c| \otimes |l_s\rangle \langle l_s|, \quad (4)$$

where W denotes the interaction strength. Throughout the remaining, we use periodic boundary conditions; i.e., $|L+1\rangle = |1\rangle$. The dimension of the full Hilbert space thus is $\mathcal{N} = L^2$. The scale of the motor current will be measured in units of the maximal group velocity $v_0 = J_c d / \hbar$.

dc-quantum current.—The mean “carrier” current is given as the speed of the motor by using the velocity operator: $\hat{v}_c(t) = i/\hbar [H_{\text{tot}}(t), \hat{x}_c]$. With $\hat{x}_c = \sum_l l_c |l_c\rangle \langle l_c|$, one finds $\hat{v}_c(t) = -i(v_0/2) \left(\sum_{l_c=1}^L e^{iA(t)} |l_c+1\rangle \langle l_c| - \text{H.c.} \right) \otimes \mathbf{1}_s$. In the quasimomentum representation with $|\kappa_l\rangle = \sum_{n=1}^L \exp(i\kappa_l n) |n\rangle$, its quantum expectation $v_c(t; t_0) = \langle \psi(t) | \hat{v}_c(t) | \psi(t) \rangle$ reads

$$v_c(t; t_0) = v_0 \sum_{l=1}^L \rho_{\kappa_l}(t; t_0) \sin(\kappa_l + A(t)), \quad (5)$$

wherein $\kappa_l = 2\pi l/L$ is the single particle quasimomentum and where we indicated its parametric dependence on the start time t_0 . Further, $\rho_{\kappa}(t; t_0) = \sum_{l_s, l_m} \langle \psi(t) | \kappa_{l_s} \rangle \otimes |\kappa\rangle \langle \kappa| \otimes \langle \kappa_{m_s} | \psi(t) \rangle$ is the quasimomentum distribution for the carrier.

The steady state regime of the motor can be characterized by the dc-component of the averaged velocity

$$v_c(t_0) := \lim_{t \rightarrow \infty} \frac{1}{t} \int_0^t v_c(s; t_0) ds. \quad (6)$$

We note that for a vector potential that is strictly linear in time t , i.e., $A(t) = \omega_B t$, providing a constant bias acting on the carrier, induces Bloch oscillations only [11]. In distinct contrast, we use here an unbiased time-dependent vector potential possessing a zero dc-component. To attain a stable asymptotic regime we use a sudden switch-on at start time t_0 of the periodically varying harmonic mixing drive [12, 15, 16]:

$$A(t) = \chi(t - t_0) [A_1 \sin(\omega t) + A_2 \sin(2\omega t + \Theta)]. \quad (7)$$

Here, $\chi(t - t_0)$ is the step function, and Θ denotes the crucial symmetry-breaking phase shift (see below) between the two harmonics which in turn yields the desired, non-vanishing dc-current.

We emphasize that with a vanishing interaction between the particles, i.e., $W = 0$, not even a finite transient current results for an initially prepared, localized carrier with zero momentum. This fact holds for *any* shape of the potential $A(t)$ [12]. This situation thus mimics the one taking place in a single-phase ac-motor: a periodically pulsating magnetic field would fail to put a

rotor from rest into rotation, unless one applies an initial kick via a starter mechanism [14]. In our setup, it is the second particle that takes over the role of a quantum starter.

Quantum current in terms of Floquet states.—The dynamics at times $t > t_0$ of the time-periodic Hamiltonian (1) can be analyzed by using the Floquet formalism [13]. The solution of the eigenproblem: $U(t, t_0) |\phi_n(t; t_0; k)\rangle = \exp(-\frac{i}{\hbar} \epsilon_n t) |\phi_n(t; t_0; k)\rangle$, with the propagator $U(t, t_0) = \mathcal{T} \exp\left(-\frac{i}{\hbar} \int_{t_0}^t H_{\text{tot}}(\tau) d\tau\right)$ (\mathcal{T} denotes the time ordering), provides the set of Floquet states, being time-periodic, i.e., with $T = 2\pi/\omega$ being the driving period, $|\phi_n(t + T; t_0; k)\rangle = |\phi_n(t; t_0; k)\rangle$. Here, $k = \sum_{l,m} \langle \phi_l | \kappa_l \rangle_s \otimes |\kappa_m\rangle_c$ is the *total* quasimomentum of the Floquet state. Due to the discrete translation invariance of the system, the total quasimomentum is conserved during the time evolution, thus serving as a quantum number. Since H_{tot} is a function of the time difference $t - t_0$ only, the quasienergies ϵ_n are independent of t_0 . The Floquet states for different start times t_0 are for a given quasienergy related by $|\phi_n(t; t_0; k)\rangle = |\phi_n(t - t_0; t_0 = 0; k)\rangle$.

We next decompose the time evolution of an initial state in the complete basis of Floquet states; i.e., $|\psi(t, t_0)\rangle = \sum_{n=1}^{\mathcal{N}} \exp(-\frac{i}{\hbar} \epsilon_n t) c_n(t_0) |\phi_n(t; t_0; k)\rangle$, where the coefficients $c_n(t_0) = \langle \phi_n(-t_0; k) | \psi(t = t_0 = 0) \rangle$ depend only on initial start time, and $|\phi_n(t; k)\rangle \equiv |\phi_n(t; t_0 = 0; k)\rangle$. Substitution of the above decomposition into (6) yields the result

$$v_c(t_0) = \sum_{n=1}^{\mathcal{N}} \bar{v}_n |c_n(t_0)|^2, \quad \bar{v}_n = \frac{1}{T} \int_0^T dt v_n(t; t_0). \quad (8)$$

Here, \bar{v}_n denotes the mean velocity of the n -th Floquet state (5). Note that the dependence of the generated dc-current on the t_0 solely stems from the coefficients $c_n(t_0)$.

Input/Output characteristics.—The mere presence of the starter is not sufficient for a motor operation. For zero-momentum initial conditions, an unbiased symmetric ac-force would launch – with equal probabilities – the system either into a clockwise (rightward) or a counterclockwise rotation (leftward motion) [15]. Thus, the *modus operandi* as a motor requires a symmetry-breaking driving field, realized here with the harmonic mixing signal. The latter knowingly may exhibit a non-vanishing nonlinear response [12, 15, 16]. Combining time-reversal operation and the complex conjugation applied to (5) with $A(t)$ in the form of (7), one can prove the (anti-) symmetric dependence of \bar{v}_n on Θ for the Floquet states with $k = 0$: $\bar{v}_n(\pi - \Theta) = \bar{v}_n(\Theta)$, $\bar{v}_n(-\Theta) = -\bar{v}_n(\Theta)$. Thus, the Floquet states with $k = 0$ possess zero mean velocities at $\Theta = 0, \pi$. Furthermore, using a similar reasoning, one finds that the set of Floquet states with nonzero k can be ordered by the parity relation, which links eigenstates with opposite quasimomenta, $\phi_n(t; t_0; -k; \Theta) = \phi_m(T - t; t_0; k; -\Theta)$, yielding $\bar{v}_n = -\bar{v}_m$. This implies that for a symmetric

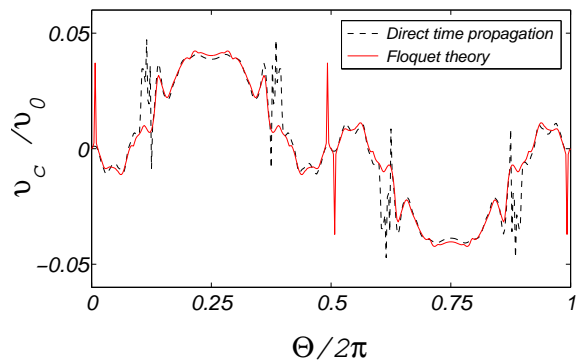


FIG. 2: (color online) Averaged motor velocity in (9) (in units of the recoil velocity $v_0 = J_c d / \hbar$) as a function of the phase shift Θ in (7) for $L = 16$. The (t_0) -averaged velocity (6) obtained by the direct time propagation of the initial state up to $200T$ (dashed line) is compared to the asymptotic dependence given by the Floquet approach (8) (red solid line). The parameters are $\hbar\omega = 0.1 \times J_c$, $A_1 = 0.5$, $A_2 = 0.25$, $W = 0.2J_c$, $J_s = J_c = J$.

(in k) initial state and $\Theta = 0, \pi$, the contributions to the dc-current of Floquet states with opposite quasimomenta eliminate each other. The same holds true for a monochromatic driving (7), with $A_2 = 0$ [15]. Shifting Θ away from $0, \pm\pi$ causes the decisive symmetry breaking and leads to the de-symmetrization of the Floquet states with $k = 0$ and consequently will violate the parity between states with opposite signs of k .

The motor speed depends on the initial conditions, which define the contributions of different Floquet states to the carrier velocity (8). We restrict our analysis to the initial state $\psi(t_0) = L^{-1/2} |l_c\rangle \otimes \sum_{l_s} |l_s\rangle$, $l_c = 1, \dots, L$, in the form of the localized carrier (at l_c) and the uniformly “smeared”, delocalized starter. Both particles have zero velocities at $t = t_0$. The asymptotic velocity typically exhibits a dependence on t_0 [18]. We first discuss the results obtained after averaging over t_0 , thus assigning a unique motor velocity value,

$$v_c = \langle v_c(t_0) \rangle_{t_0} = 1/T \int_{t_0}^{T+t_0} v_c(t_0) dt_0, \quad (9)$$

for fixed system parameters.

Figure 2 depicts the dependence of the average motor velocity on Θ . The results obtained by direct time propagation of the initial state and averaged over t_0 (dashed line) are superimposed by those calculated via the Floquet formalism (8) (solid line). The agreement between the two curves is satisfactory but not perfect: This is so because the sharp peaks on the asymptotic current (8) are not resolved by the system’s maximal evolution time $t = 200T$. These peaks can be associated with *avoided crossings* between two quasienergy levels [15]. These avoided crossing cause a strong current enhancement if one of the interacting, and transporting eigenstate over-

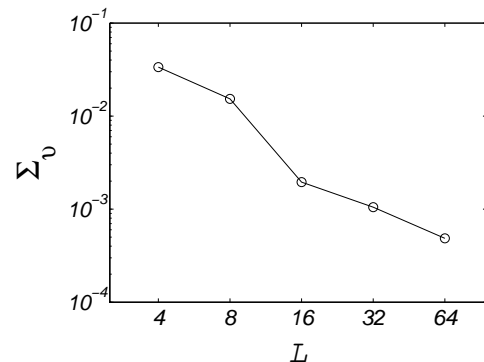


FIG. 3: Dispersion of the motor velocity (10) vs. the number of lattice sites L . Here $\Theta = \pi/2$, and the other parameters are the same as in Fig. 2.

laps significantly with an initial non-transporting state of the motor. We further found that the dependence of the motor velocity $v_c(t_0)$ in (6) on t_0 increasingly disappears upon increasing the size L (not shown).

To provide a quantitative estimate, we evaluated the dispersion of the current (8) with respect to t_0 , i.e.,

$$\Sigma_v = \sqrt{\langle v_c(t_0)^2 - \langle v_c(t_0) \rangle_{t_0}^2 \rangle_{t_0}}. \quad (10)$$

As shown in Fig. 3 this dispersion decays with increasing L , being rather faint at $L \simeq 10$. For sizes $L \gtrsim 10$ the carrier gains approximately an identical asymptotic velocity, independently on the initial start time t_0 . The weak dependence of the coefficients $c_n(t_0)$ on t_0 (8) follows from the nature of the Floquet states; i.e., their decomposition in the basis of Bloch waves tends to become time-independent with increasing the lattice size L .

Load characteristics.—The analysis based on Eqs.(1 - 3, 7) has been for a free rotator. In order to qualify for a genuine motor device, the engine must be able to operate under an applied load. The load is introduced as the bias $\omega_B t$, being added to the vector potential $A(t)$. All the information about transport properties can be extracted by using again the Floquet formalism, provided that the ac-driving and the Bloch frequencies are mutually in resonance [19], i.e. $q\omega = r\omega_B$, where r and q are co-prime integers. Figure 4a depicts the spread of the motor velocities of Floquet states for different bias values. There are two remarkable features. First, the spectrum of velocities is symmetric around $\omega_B = 0$. This follows because of the specific choice of the phase shift at $\Theta = \pi/2$. Second, while some Floquet states provide a transport velocity along the bias, others correspond to the up-hill motion, against the bias. Therefore, a stationary transport in either direction is feasible. Figure 4b shows the dependence of the asymptotic motor speed for the above described initial condition “localized carrier/delocalized starter”. The load characteristics exhibits a discontinuous, fractal structure and, in distinct contrast to the clas-

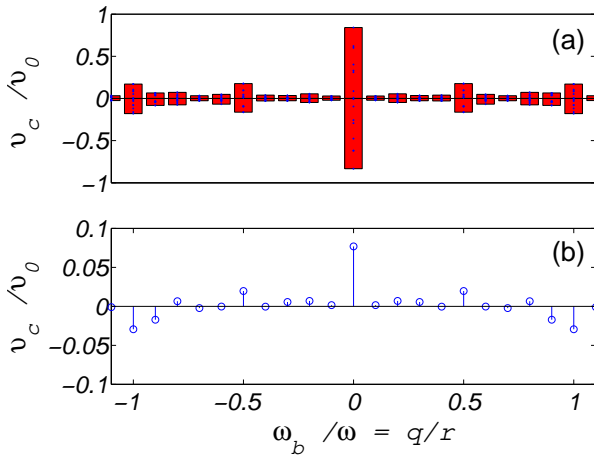


FIG. 4: (color online) The average motor velocity *vs.* the load (in units of ω). (a) The range of values v_c for a single Floquet state out of the complete set. (b) The average motor velocity for “resonance” driving and an initial condition “localized carrier/delocalized starter” ($r = 10$). The parameters are $W = 0.2J_c$, $J_s = J_c = J$, $\hbar\omega = 0.1J_c$, $A_1 = 0.5$, $A_2 = 0.25$, $\Theta = \pi/2$, and $L = 4$.

sical case [20], it cannot be approximated by a smooth curve. This is a direct consequence of the above mentioned resonance condition.

Experimental realizations.—For an experimental realization of this quantum atom motor the following features should be respected: (i) In the case of the setup “carrier with a spin/spinless starter”, the carrier should assume a magnetic number $m_F \geq 2$ [6], to efficiently induce the ac-field amplitudes $A_{1,2}$. (ii) Because in the tight-binding approximation the maximal amplitude of the tunneling is limited from above, $J_c \lesssim J_{max} = 0.13E_0$, for ${}^6\text{Li}$ atom, the lattice spacing $d \sim 10\mu\text{m}$ [7], and $\hbar\omega = 0.1J_c$ (used in the calculations), the driving frequency ω should be less than 2Hz. Then, the time required to launch the motor (i.e., to approach the asymptotic velocity value) is around a minute. This seemingly is beyond the state of the art for the coherence time in present-day experimental setups. Nevertheless, further focusing of the laser beam can decrease the lattice constant d , thereby decreasing the launch time to experimentally accessible coherence times around 10 seconds [21]. This implies reasonably long observation times that are possible even with existing experimental setups in use [7].

Conclusions.—We studied a quantum ac-motor made of the two species of ultracold interacting atoms, i.e. a “carrier” and a “starter”, moving in a ring-shaped trapping potential. For zero-momentum initial conditions the asymptotic carrier velocity does not depend on the switch-on time t_0 of the ac-drive. A natural question that arises is: – what about the averaged starter velocity v_s ? We find that the latter sensitively depends on the system parameters: It can either be very small compared to the carrier’s velocity or also larger than v_c . In short, the

starter can move co-directionally or contra-directionally to the carrier motion. Moreover, an extension of our motor setup to several interacting bosons (i.e. a finite bosonic “heat bath”) presents an intriguing perspective.

We acknowledge I. V. Ponomarev for providing us with the illustration shown in Fig.1. This work was supported by the DFG through grant HA1517/31-1 and by the German Excellence Initiative “Nanosystems Initiative Munich (NIM)”.

-
- [1] The conversion of electrical energy into mechanical work by electromagnetic means was devised by Michael Faraday in 1821. The first operating electric motor was demonstrated by Ányos Jedlik in 1828.
 - [2] J. G. Korvink and O. Paul, *Microelectromechanical systems* (Norwich, New-York, Springer, 2006).
 - [3] A. M. Fennimore, Nature **424**, 408 (2003); D. L. Fan, F. Q. Zhu, R. C. Cammarata, and C. L. Chien, Phys. Rev. Lett. **94**, 247208 (2005).
 - [4] R. A. van Delden *et al.*, Nature **437**, 1337 (2005); E. R. Kay, D. A. Leigh and F. Zerbetto, Angew. Chem. Int. Ed. **46**, 72 (2007); G. S. Kottas, L. I. Clarke, D. Horinek, and J. Michl, Chem. Rev. **105**, 1281 (2005).
 - [5] O. Morsch and M. Oberthaler, Rev. Mod. Phys. **78**, 179 (2006).
 - [6] L. Amico, A. Osterloh, and F. Cataliotti, Phys. Rev. Lett. **95**, 063201 (2005).
 - [7] S. Franke-Arnold *et al.*, Opt. Exp. **15**, 8619 (2007).
 - [8] For example, it can be bosonic ${}^{174}\text{Yb}$ atom, prepared in spinless ground state plus fermionic ${}^{171}\text{Yb}$ atom, see K. Honda *et al.*, Phys. Rev. A **66**, 021401(R) (2002); or bosonic ${}^{87}\text{Rb}$ plus fermionic ${}^6\text{Li}$, see C. Silber *et al.*, Phys. Rev. Lett. **95**, 170408 (2005).
 - [9] S. Viefers, P. Koskinen, P. Singha Deo, and M. Manninen, Physica E **21**, 1 (2004).
 - [10] A. E. Leanhardt *et al.*, Phys. Rev. Lett. **89**, 190403 (2002).
 - [11] A. V. Ponomarev, J. Madronero, A. R. Kolovsky, and A. Buchleitner, Phys. Rev. Lett. **96**, 050404 (2006).
 - [12] I. Goychuk and P. Hänggi, J. Phys. Chem. B **105**, 6642 (2001).
 - [13] M. Grifoni and P. Hänggi, Phys. Rep. **304**, 279 (1998).
 - [14] A. Hughes, *Electric motors and drives* (Newnes, London, 3rd. ed., 2006).
 - [15] S. Denisov, L. Morales-Molina, S. Flach, and P. Hänggi, Phys. Rev. A **75**, 063424 (2007).
 - [16] P. H. Jones, M. Goonasekera, and F. Renzoni, *ibid.* **93**, 073904 (2004); R. Gommers, S. Bergamini, and F. Renzoni, *ibid.* **95**, 073003 (2005); P. Sjolund *et al.* Phys. Rev. Lett. **96**, 190602 (2006).
 - [17] B. W. Shore, Phys. Rev. A **17**, 1739 (1978).
 - [18] In a single-particle quantum ratchet the asymptotic current may even change sign upon variation of t_0 [15].
 - [19] M. Glück, A. R. Kolovsky, and H. J. Korsch, Phys. Rep. **366**, 103 (2002).
 - [20] M. Kostur *et al.*, Physica A **371**, 2024 (2006).
 - [21] M. Gustavsson *et al.*, Phys. Rev. Lett. **100**, 080404 (2008).